Why is it difficult to grow spontaneous ZnO nanowires using molecular beam epitaxy?

Vincent Sallet, Christiane Deparis, Gilles Patriarche, Corinne Sartel, Gaelle Amiri, Jean-Michel Chauveau, Christian Morhain, Jesus Zuñiga Perez

Why is it difficult to grow spontaneous ZnO nanowires using molecular beam epitaxy?

Vincent Sallet[1], Christiane Deparis[2], Gilles Patriarche[3], Corinne Sartel[1], Gaelle Amiri[1], Jean-Michel Chauveau[2], Christian Morhain[2], Jesus Zuñiga Perez[2].

[1] Université Paris-Saclay, CNRS, Université de Versailles St Quentin en Yvelines, Groupe d'Etude de la Matière Condensée (GEMAC), 45 avenue des Etats-Unis, 78035 Versailles, France.
[2] Université Côte d'Azur, CNRS, CRHEA, Rue B. Gregory, 06905 Sophia Antipolis Cedex, France.
[3] Université Paris-Saclay, CNRS, Centre de Nanosciences et de Nanotechnologies (C2N), 10 Boulevard Thomas Gobert, 91120, Palaiseau, France.

E-mail: vincent.sallet@uvsq.fr

Received xxxxxx
Accepted for publication xxxxxx
Published xxxxxx

Abstract

Surface diffusion is known to be of prime importance in the growth of semiconductor nanowires. In this work, we used ZnMgO layers as markers to analyze the growth mechanisms and kinetics during the deposition of ZnMgO/ZnO multilayered shells by molecular beam epitaxy on previously grown ZnO nanowire cores (so called core-shell heterostructures). Specifically, the influence of the O_2 flow sent into the plasma cell on the adatom surface mobility was investigated. By carefully measuring the growth rate on the lateral facets as well as on the top of the nanowires, it is concluded that the surface diffusion length of adatoms, within the used MBE growth conditions, is very low. Such poor surface mobility explains why so few works can be found related to the spontaneous growth (without catalyst) of ZnO nanowires by MBE, contrary to other deposition techniques.

Keywords: surface diffusion, ZnO nanowires, molecular beam epitaxy, transmission electron microscopy, core-shell heterostructures

1. Introduction

Semiconductor nanowires (NWs) have received considerable attention for almost two decades, and are still the focus of a great interest for future applications in electronics, optoelectronics, energy harvesting or sensor devices. Among the studied materials, zinc oxide (ZnO) offers a large variety of nanostructures including nanowires, nanobelts, and nanoribbon [1]. Indeed, regarding the particular case of ZnO nanowires vertically grown on a substrate such as sapphire, silicon or glass, the panel of growth techniques allowing their fabrication with high structural and optical quality even at low cost, is very rich. Vapor transport [2], pulsed laser deposition [3], metalorganic chemical vapor deposition (MOCVD) [4], hydrothermal [5], and electrodeposition [6] allow the spontaneous growth (vapor-solid process, VS) without the assistance of a metal catalyst (so called vapor-liquid-solid, VLS, or vapor-solid-solid, VSS). Surprisingly, very few articles have been published on molecular beam epitaxy (MBE) non-catalyzed growth of ZnO NWs [7,8].

In VS, VLS or VSS growth of semiconductor nanowires, surface diffusion of adatoms plays a major role. Dubrovskii *et al* [9] as well as Harmand *et al* [10] have thoroughly investigated the nanowire growth and have proposed theoretical models to describe the involved mechanisms,

taking into account adsorption of atoms, desorption, diffusion and incorporation. Furthermore, stress-driven nucleation [11] or phase transition from zinc-blende to wurzite [12] have been studied. In the literature, several experiments were conducted to measure the surface diffusion length of adatoms, which is known to be strongly growth condition dependent, as well as facet orientation dependent [13]. Galopin *et al* [14] used AlN markers periodically introduced in GaN NWs to study the growth kinetics, and assessed a gallium diffusion length λ_s = 40 nm on the sidewalls of the NW. In a different manner, Jensen *et al* [15] used electronic lithography to pattern InAs substrates with gold droplets, and subsequently selectively grow InAs NWs below the catalyst. The authors evaluated indium diffusion lengths on (111)B substrate and {110} NWs facets : $\lambda_{(111)B}$ = 650 nm and $\lambda_{\{110\}}$ > 10µm. Regarding zinc diffusion length, Kim *et al* [16] fabricated ZnO nanowires on GaN/sapphire by vapor transport. Studying the correlation between length and diameter, they suggest that the diffusion length on a non-polar surface such as {10-10} sidewalls is more than 10 µm, but is less than 40 nm on a polar surface like (0001) NW tip.

In the MOCVD process of ZnO, the dominant parameter appearing to trigger the growth mode transition from 2D layer to 1D nanostructures is the O/Zn ratio ($R_{O/Zn}$) defined by the partial pressures of zinc and oxygen precursors [17]. It is suggested that high oxygen concentration in the gas phase tends to limit the diffusion of Zn atoms and favors the 2D growth. This assumption is supported by the work of Chen *et al* [18] where plasma-assisted molecular beam epitaxy has been used, and it was also reported that under O-rich condition, i.e. high $R_{O/Zn}$, oxygen atoms on the growing surface stabilize the incoming Zn atoms.

In this work we studied the MBE growth of ZnMgO/ZnO multilayered shells deposited on previously fabricated ZnO nanowires (these latter by MOCVD), so called "core-shell structures". The motivation was two-fold : i) achieve high quality heterostructures with abrupt interfaces, where ZnMgO layers can act as markers [14,19], and ii) discuss the growth mechanisms, in particular the mobility of Zn adatom as a function of a specific growth condition, namely the oxygen exposure flow.

2. Methodology and experimental details

Core-shell ZnMgO/ZnO samples have been fabricated following a two-step process. First, ZnO nanowires were grown on A(11-20) sapphire substrates by MOCVD in a horizontal quartz reactor, using diethylzinc (DEZn) and nitrous oxide (N_2O) sources, and helium as carrier gas. Substrate temperature was 850°C (RF heating), reactor pressure 50 torr, for a growth duration of 30 min. This process typically allows the achievement of vertically aligned ZnO nanowires with length of ~5-7 µm and diameter ~100 nm. Subsequently, ZnMgO/ZnO multilayered shells were deposited on such nanowires using a RIBER EPINEAT system equipped with an oxygen RF plasma cell and using elemental 6N Zn and Mg effusion cells designed to be used with oxygen. The Zn and Mg beam fluxes, deduced from the measurements of an ionization gauge, were φ_{Zn}=1.1x10^{14} atoms/cm^2.s and φ_{Mg}= 5.4x10^{12} atoms/cm^2.s. O_2 flow sent in the plasma source was varied in the range 0.3 – 0.9 sccm, with power of 420 W. With such variation of the oxygen exposure, we modified the growth conditions and thus we expected to influence the growth mechanisms. Growth temperature, measured at the backside of the substrate with a pyrometer, was set at 450°C. Within such conditions, calibration samples give a growth rate of 0.07 nm/sec for 2D ZnO films on M-plane ZnO substrates, and the Mg content of the $Zn_{1-x}Mg_xO$ alloy is around 15%.

Two dedicated samples have been produced and characterized for this study. An illustration is given in figure 1a for more clarity. Firstly, a reference structure S1 composed of ZnO NW cores coated with three pairs of ZnMgO/ZnO layers was made. Hence, the global shell has six components numbered from n°1 (first ZnMgO) to n°6 (last ZnO). The growth duration was the same for all ZnMgO layers (n°1, n°3 and n°5, the time corresponds to 10 nm in 2D growth mode), while it was progressively increased for the ZnO layers (n°2, n°4, and n°6, the times correspond to 10 – 20 – 30 nm in 2D growth mode). This reference sample is grown for two purposes : i) check the abruptness and contrast between ZnO and ZnMgO (so that the alloyed layer can be efficiently used as a marker), and ii) check that the growth rate is constant for ZnO layers whatever the number (in other words : the order of growth), and so for ZnMgO markers. Then, in order to investigate the effect of the O_2 flow on the adatom surface diffusion and consequently on the growth rate, the same kind of structure was made, and labeled S2. But in that case, for the three pairs of ZnMgO/ZnO layers the growth proceeded as follows : fixed duration (corresponding to 10 nm ZnMgO and 25 nm ZnO in 2D growth mode), and variable O_2 flow of 0.3, 0.6, 0.9 sccm for pairs n°1-2, n°3-4, and n°5-6 respectively.

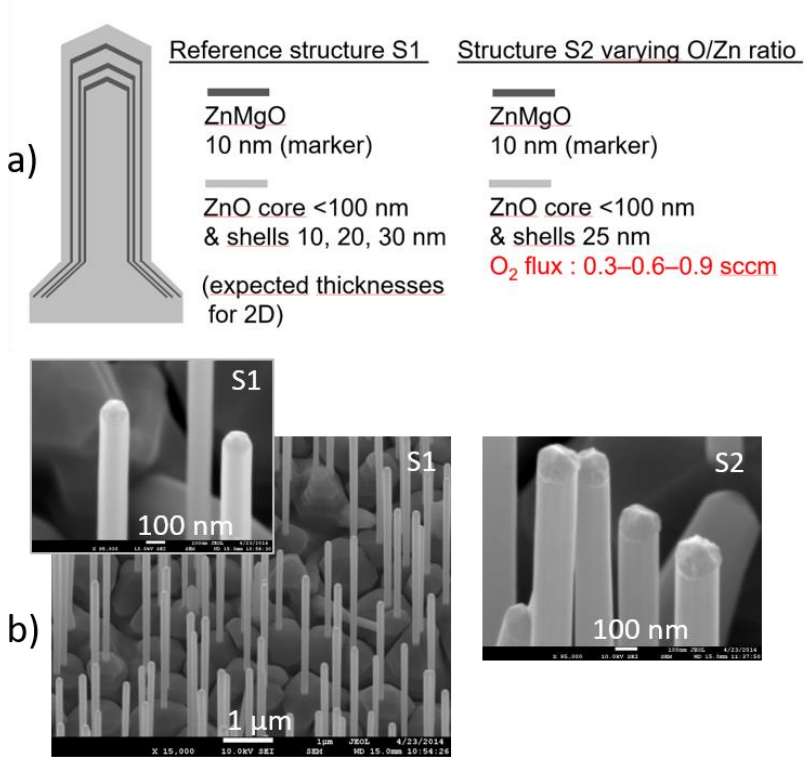

Figure 1 : a) schematic structure, and b) SEM images of samples S1 and S2.

The morphology of the nanostructures has been characterized by scanning electron microscopy (SEM, JEOL 7001). Nanowires were previously scratched and spread on the carbon membrane of a TEM copper grid. Scanning transmission electron microscopy (STEM) observations were made on a Titan Themis 200 microscope (FEI/ Thermo Fischer Scientific) equipped with a geometric aberration corrector on the probe. This microscope is also equipped with the "Super-X" systems for EDX analysis with a detection angle of 0.9 steradian. The observations were conducted at 200 kV with a probe current of about 70 pA and a half-angle of convergence of 24 mrad. HAADF-STEM images were acquired with a camera length of 110 mm (inner/outer collection angles are respectively 69 and 200 mrad).

3. Results

Figure 1b gathers SEM images of samples S1 and S2 after the deposition of the multilayered shell. It appears that core nanowires are homogeneously coated from the bottom to the top. It can be roughly measured that the diameter increased to 150 nm for sample S1 and 180 nm for sample S2. The diameter of the initial core ZnO nanowires being ~100 nm, this means that approximately 25 nm and 40 nm of shell have been deposited on the lateral facets of S1 and S2, respectively, which will be confirmed by STEM analysis.

For careful investigation of the sample structure that will allow the discussion on growth mechanisms and kinetics, STEM experiments were carried out. Figures 2a and 2b present dark field images of the upper part of the two structures. For sample S1, it is remarkable that each layer making the shell can be distinguished on the lateral facets as well as on the top facets. The contrast between ZnMgO and ZnO allows to separate the binary from the ternary material. The EDX image that maps the Mg incorporation confirms the localization of ZnMgO markers in the structure (figure 2c). Mg concentration x_{Mg} is measured between 11 and 14% in the $Zn_{1-x}Mg_xO$ alloy. Sample S2 also presents a nice lateral ZnMgO/ZnO stacking. One will observe that the top of the nanowire is nevertheless more disturbed. Examining the details, it is noted that the first layers n°1-2-3-4 have actually achieved a good conformal coating of the topmost facets, but the deposition of the two layers n°5-6 has led to uncontrolled 3D growth. This could be explained by the high O_2 flow used for this last pair, i.e. growth conditions far from the optimized ones, which would bring instability in the growth (however localized on the tip of the nanowire). A high resolution STEM image is also given in figure 2d as an example. It is indeed convincing that such images enable the accurate measurement of the thickness of the six layers composing the shell, and consequently, the determination of the growth rate as a function of the growth conditions (time, O_2 flow) at different locations of the nanowire. We notice that due to exposure

conditions to the atom flux, the thickness is much less on the sides of the nanowires than the expected one on the 2D substrate surface. For example, the ZnMgO marker thickness which is 10 nm on 2D substrates falls to 3 nm on the NW lateral facets. We will later focus on that point in the discussion section.

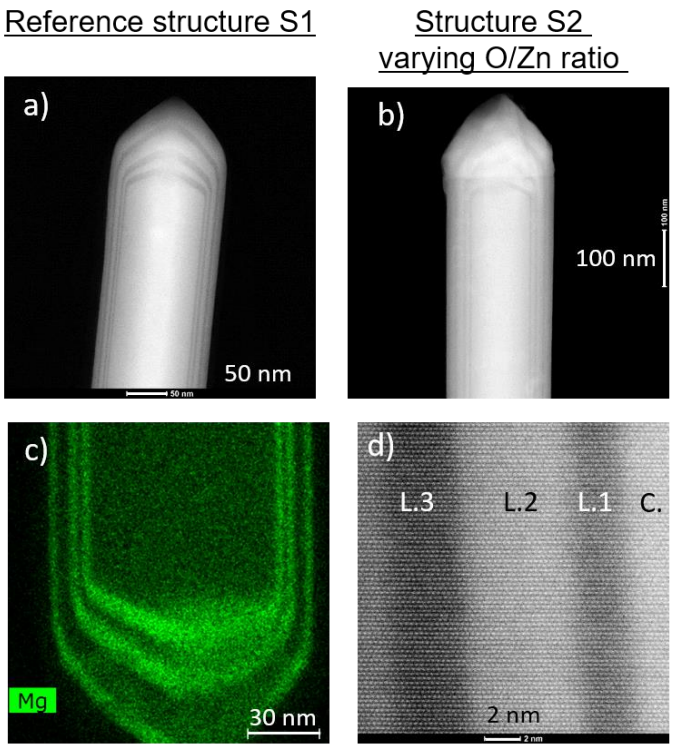

Figure 2 : a) upper part of reference sample S1, b) upper part of sample S2 varying O_2 flow, c) Mg EDX mapping of S1, and d) high resolution image from S2. C., L.1, L.2 and L.3 refers to ZnO core, ZnMgO layer 1, ZnO layer 2 and ZnMgO layer 3, respectively.

Following such methodology, we plotted the growth rate related to each ZnMgO and ZnO layer, both on the lateral facets and on the summit of the core-shell structure. Measurements followed the dashed red lines indicated in the figure 3. This shows that we are indeed referring to axial and radial growth rates.The images from which measurements have been done are given in figure 3a and 3b. In the case of sample S2 exhibiting fuzzy top, magnesium EDX mapping helped in the thickness assessment. The last pair of ZnMgO/ZnO grown with 0.9 sccm was hardly measureable at the top the structure, and layer 6 thickness could not be assessed. For both S1 and S2 samples, the radial growth rate was measured to be constant along the nanowire, so that the overall nanowire radius remains rather constant. High resolution STEM images enabled the thickness measurement with an error from 0.5 to 1 nm on the lateral facets. Decreasing with the layer thickness, the error bar for radial growth rate is between 0.002 and 0.004 nm/sec. The measurement on the summit point of the nanowire is less accurate, especially for structure S3 with fuzzy tip. The axial growth rate error is estimated between 0.01 and 0.02 nm/sec.

For the reference sample S1, the growth rate is clearly kept constant regardless of the layer number and the material, with a value of 0.02 nm/sec (figure 3c). One will note that the error bar is larger for ZnMgO layers since thicknesses are thinner. In addition, we can comment at this stage that equal growth rate for ZnO and ZnMgO using same MBE conditions means the layers were grown in element II-rich regime, i.e. limited by the oxygen flux. In figure 3c, the same trend is observed regarding the growth rate on the summit of the nanowire, with a constant value of 0.07 nm/sec. The ratio $\frac{V_g\,(\mathrm{top})}{V_g\,(\mathrm{lat})}$ between the lateral facets and top of the nanowire is then 3.5.

In the case of sample S2, a quite different behavior is observed in the figure 3d. The lateral growth rate increases for each pair of ZnMgO/ZnO layers when the O_2 flow is varied. 0.02, 0.027, and 0.035 nm/sec are measured corresponding to O_2 flows of 0.3, 0.6 and 0.9 sccm respectively. Even though

accurate assessment is more difficult, the growth rate on the top of sample S2 also appears enhanced with the increase of the O_2 flow.

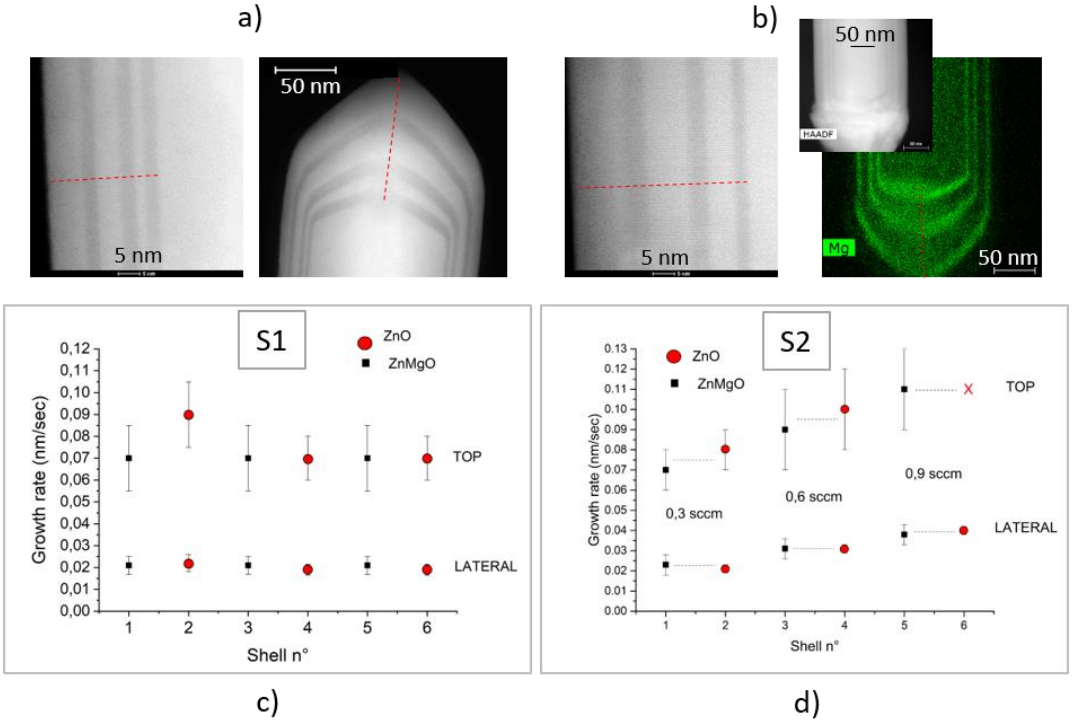

Figure 3 : a) STEM images of S1 from which layer thicknesses were measured (dashed red lines). b) STEM images of S2, and Mg EDX mapping which also helped in thickness measurement c,d) growth rates as a function of the shell number

4. Discussion

We can first emphasize that the reference sample S1 shows constant growth rate for all layers. Consequently, there is no influence of the shell deposition order (e.g. layer 2 shows the same growth rate as layer 6), neither of the growth time. This enables the relevant analysis of sample S2 and verifies that growth rate variations in S2 are only due to O_2 flow variation. That will permit consideration on the growth mechanisms to be done.

ZnO nanowires are commonly grown following a catalyzed mode (e.g. induced by a Au-droplet [20]), or a spontaneous mode without the assistance of a catalyst. This spontaneous mode is not a self-catalyzed process in the sense of GaAs NWs growth mode, where a Ga droplet is previously formed on the substrate and acts as a catalyst which is continuously feeded [21]. Indeed, no Zn or ZnO_x droplets have ever been observed by TEM in our MOCVD nanowires, even if cooling down after growth was performed keeping DEZn exposure flow, without N_2O flow, hence giving more chance to an hypothetic Zn droplet to remain on the tip. Therefore, the spontaneous fabrication of ZnO NWs is driven by surface energies, kinetics, incorporation of adatoms on specific sites depending on the surface orientation and polarity, and surface diffusion which plays a major role as mentioned in the introduction. In our growth experiments, shells have been achieved by MBE to cover previously fabricated ZnO NWs cores. Contributions to lateral and top deposition can be given by : i) adatoms directly impinging the growing surfaces, and ii) adatoms diffusing from the substrate and/or the lateral facets as modeled by Dubrovskii [9]. As mentioned in the introduction, Chen and co-authors [18] have investigated the plasma-assisted MBE growth of ZnO. They reported a significant damping of the RHEED oscillations when increasing the O_2 flow, from 1.5 to 2.5 sccm, associated with the evolution of the layer morphology observed by AFM, and concluded that oxygen stabilizes mobile Zn adatoms. This situation is indeed similar to the growth of GaAs, for which the diffusion length of Ga atom on GaAs has been considered inversely proportional to the As pressure, at fixed substrate temperature [13].

This leads to the focus on the lateral growth rate of sample S2. Interestingly, it is measured to increase with O_2 flow. Taking into account the previous considerations on NW growth mechanisms, we would expect for this sample S2 that

the Zn adatoms mobility would decrease varying the O_2 flow from 0.3 to 0.9 sccm. If this occurs, the contribution of adatoms diffusing from the substrate and participating to the lateral and axial growths would be drastically reduced. Then, such phenomenon would lead to a decrease of the shell growth rate. In this work, our results strongly disagree with this expectation as, on the contrary, both lateral and top growth rates increase. The explanation is that the O-limited regime was kept in our experiments. As is typically the case for layers grown on 2D substrates, increasing the O flux (Zn flux) in Zn-rich (O-rich) conditions makes the growth rate increase. Therefore, there is a strong assumption that Vg is only due to atoms from the effusion cell directly impinging the nanowire and incorporated at (or very close to) the adsorption site. To confirm this, a simple calculation can be done based on geometrical considerations. The schematic in figure 4 illustrates the beam exposure in the MBE chamber. The angle between the atom flux φ_0 and the substrate surface is approximately 50°, and the rotation speed of the substrate holder is around 4 rpm.

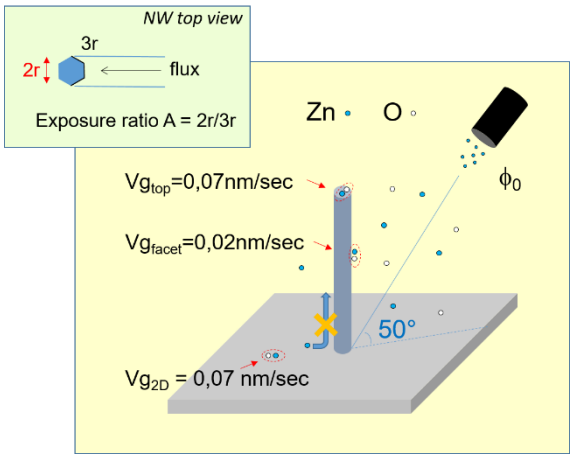

Figure 4 : MBE configuration and growth model

The flux of atoms impinging the 2D substrate surface is expressed by :

$$\varphi_{2D} = \varphi_0 \sin 50°$$

Taking into account that, at any time, half of the lateral surface of the NW is not exposed, the Zn flux on the rotating facet is given by :

$$\varphi_{lat} = \frac{1}{2}.A.\varphi_0 \cos 50°$$

with A the exposure ratio between a flat surface perpendicular to the flux, and the surface of the hexagonal NW exposed to the same flux. A can be approximated as $\frac{2rL}{3rL} = 2/3$ where r is the nanowire radius and L its length (see insert in figure 4).

If we assume that only adatoms hitting the considered area (NW sides, NW top, substrate) participate to the growth, and that the diffusion of adatoms is very weak so that they are rapidly incorporated in the growing crystal, then we can consider the growth rate proportional to the atom flux. Thus we can calculate a growth rate ratio between 2D substrate surface and facet, $\frac{V_g\,(2D)}{V_g\,(lat)}$, equal to the flux ratio $\frac{\varphi_{2D}}{\varphi_{lat}} = 3.\tan 50° = 3.6$.

Next, if we consider the experimental data, the calibration layer on M-plane ZnO substrate gives Vg(2D)=0.07 nm/sec. We note that this value is equal to the measured value on the top of the nanowires Vg(top). This is a first indication that only adatoms impinging the tip of the nanowire are incorporated at this location, without any additional contribution of the lateral facets and substrate diffusion. In the previous section, using TEM, we also measured the growth rate on the sides of the nanowires , Vg(lat) with a value of 0.02 nm/sec, which gives an experimental ratio $\frac{V_g\,(2D)}{V_g\,(lat)}$ of 3.5, very close the calculated ratio of 3.6. Hence, the experimental results agree with the growth model and support the conclusion that within the investigated MBE growth conditions, the mobility of Zn adatoms is very low, below a few tens of nanometers. This low mobility could be explained by the moderate temperature used in our experiments (450°C) and, by increasing it, we may enhance surface diffusion. MBE growth conditions have been extensively studied for more than two decades. The investigated parameters include substrate temperature and Zn- or O- rich regimes [22,23,24]. It is interesting to note that, contrary to what is observed in MOCVD growth [17], using high temperature and Zn-rich conditions the morphology of 2D layers does not evolve towards nanorods or nanowires. Indeed, no transition from 2D to 1D growth has been reported without assistance of a metal catalyst. In their article [25], Hong *et al* recorded RHEED oscillations at different substrate temperatures in the range 400-700°C, during the growth of ZnO by plasma assisted MBE. The authors observed faster oscillation damping at high temperatures and attributed such behavior to the growth mode transition from 2D nucleation to step-flow mode. Therefore, one can assume that the mobility of Zn atoms increased to allow the diffusion towards the closest surface step (a few tens to a few hundreds of nm, depending on the substrate miscut). However, we believe such enhancement is not sufficient to achieve the spontaneous 1D growth of ZnO nanowires, which requires diffusion length in the micrometer range.

Furthermore, another parameter may be taken into account to explain why it is difficult to grow spontaneous ZnO nanowires by MBE, namely the sticking coefficient of zinc, which has been reported to decrease as a function of the temperature. Precisely, it was shown to drop from 0.2 to 0.1 in the temperature range 500-700°C [26], and it most probably continues to decline above 700°C. Consequently, such low Zn

sticking coefficient at high temperatures may impede to achieve high concentration of mobile zinc atoms on the growing surface, which is a necessary condition to growth nanowires.

Interestingly, with vapor phase methods, lots of works have demonstrated the growth of spontaneous ZnO NWs at temperatures similar to the one that was used in this work (450°C) and even below, with O_2 as oxygen source [27]. One explanation could be given by considering the highly reactive nature of O-species supplied by the plasma cell. Such species would strongly react with Zn adatoms on the growing surface, thus impeding their diffusion on the substrate surface and along the sides of the nanowire. This assumption is supported by the work of Izyumskaya *et al* [28] who also studied ZnO growth on sapphire by MBE, between 450 and 650°C, but using H_2O_2 oxygen source instead of O-plasma. Noticeably, on the SEM image of the ZnO layer grown at high temperature, a rough 3D surface is observed with what appears to be short nanorods (~100 nm long). This suggests an increase of the mobility by changing the oxygen source.

5. Conclusion

Surface diffusion of adatoms was investigated by conducting the MBE growth of ZnMgO/ZnO core/shell 1D heterostructures, and further analyzing the samples by STEM. Using the ZnMgO alloy a marker to accurately measure the growth rate on the lateral and top facets of the nanowire, we infer that such surface diffusion is very low for ZnO within the used growth conditions. Interestingly, our observations help to understand why so few articles can be found as regards ZnO nanowires grown by MBE without the assistance of a catalyst. To the best of our knowledge, the only work that presents significant spontaneous 1D growth is the one of Pietrzyk *et al* [7], where a very dense array of ZnMgO nanocolumns is shown.

References

[1] Z. L. Wang, "Zinc oxide nanostructures: growth, properties and applications," Journal of Physics: Condensed Matter **16**(25), R829 (2004).

[2] A. C. Mofor, A. S. Bakin, A. Elshaer, D. Fuhrmann, F. Bertram, A. Hangleiter, J. Christen, and A. Waag, "Vapour transport growth of ZnO nanorods," Applied Physics A **88**(1), 17–20 (2007).

[3] J. Zúñiga-Pérez, A. Rahm, C. Czekalla, J. Lenzner, M. Lorenz, and M. Grundmann, "Ordered growth of tilted ZnO nanowires: morphological, structural and optical characterization," Nanotechnology **18**(19), 195303 (2007).

[4] G. Perillat-Merceroz, R. Thierry, P.-H. Jouneau, P. Ferret, and G. Feuillet, "Compared growth mechanisms of Zn-polar ZnO nanowires on O-polar ZnO and on sapphire," Nanotechnology **23**(12), 125702 (2012).

[5] V. Consonni, E. Sarigiannidou, E. Appert, A. Bocheux, S. Guillemin, F. Donatini, I.-C. Robin, J. Kioseoglou, and F. Robaut, "Selective Area Growth of Well-Ordered ZnO Nanowire Arrays with Controllable Polarity," ACS Nano **8**(5), 4761–4770 (2014).

[6] R. Tena-Zaera, J. Elias, C. Lévy-Clément, I. Mora-Seró, Y. Luo, and J. Bisquert, "Electrodeposition and impedance spectroscopy characterization of ZnO nanowire arrays," physica status solidi (a) **205**(10), 2345–2350 (2008).

[7] M. A. Pietrzyk, M. Stachowicz, A. Wierzbicka, P. Dluzewski, D. Jarosz, E. Przezdziecka, and A. Kozanecki, "Growth conditions and structural properties of ZnMgO nanocolumns on Si(111)," Journal of Crystal Growth **408**, 102–106 (2014).

[8] M. S. Kim, G. Nam, and J.-Y. Leem, "Photoluminescence Studies of ZnO Nanorods Grown by Plasma-Assisted Molecular Beam Epitaxy," Journal of Nanoscience and Nanotechnology **13**(5), 3582 (2013).

[9] V. G. Dubrovskii, G. E. Cirlin, I. P. Soshnikov, A. A. Tonkikh, N. V. Sibirev, Yu. B. Samsonenko, and V. M. Ustinov, "Diffusion-induced growth of GaAs nanowhiskers during molecular beam epitaxy: Theory and experiment," Phys. Rev. B **71**(20), 205325 (2005).

[10] J.-C. Harmand, F. Glas, and G. Patriarche, "Growth kinetics of a single $InP_{1-x}As_x$ nanowire," Phys. Rev. B **81**(23), 235436 (2010).

[11] V. G. Dubrovskii, N. V. Sibirev, X. Zhang, and R. A. Suris, "Stress-Driven Nucleation of Three-Dimensional Crystal Islands: From Quantum Dots to Nanoneedles," Crystal Growth & Design **10**(9), 3949–3955 (2010).

[12] F. Glas, J.-C. Harmand, and G. Patriarche, "Why Does Wurtzite Form in Nanowires of III-V Zinc Blende Semiconductors?," Phys. Rev. Lett. **99**(14), 146101 (2007).

[13] T. Takebe, M. Fujii, T. Yamamoto, K. Fujita, and T. Watanabe, "Orientation-dependent Ga surface diffusion in molecular beam epitaxy of GaAs on GaAs patterned substrates," Journal of Applied Physics **81**(11), 7273–7281 (1997).

[14] E. Galopin, L. Largeau, G. Patriarche, L. Travers, F. Glas, and J. C. Harmand, "Morphology of self-catalyzed GaN nanowires and chronology of their formation by molecular beam epitaxy," Nanotechnology **22**(24), 245606 (2011).

[15] L. E. Jensen, M. T. Björk, S. Jeppesen, A. I. Persson, B. J. Ohlsson, and L. Samuelson, "Role of Surface Diffusion in Chemical Beam Epitaxy of InAs Nanowires," Nano Lett. **4**(10), 1961–1964 (2004).

[16] D. S. Kim, U. Gösele, and M. Zacharias, "Surface-diffusion induced growth of ZnO nanowires," Journal of Crystal Growth **311**(11), 3216–3219 (2009).

[17] D. N. Montenegro, A. Souissi, C. Martínez-Tomás, V. Muñoz-Sanjosé, and V. Sallet, "Morphology transitions in ZnO nanorods grown by MOCVD," Journal of Crystal Growth **359**, 122–128 (2012).

[18] Y. Chen, H.-J. Ko, S.-K. Hong, T. Yao, and Y. Segawa, "Morphology evolution of ZnO(000 $\bar{1}$) surface during plasma-assisted molecular-beam epitaxy," Applied Physics Letters **80**(8), 1358–1360 (2002).

[19] R. Songmuang, T. Ben, B. Daudin, D. González, and E. Monroy, "Identification of III–N nanowire growth kinetics via a marker technique," Nanotechnology **21**(29), 295605 (2010).

[20] V. Sallet, C. Sartel, C. Vilar, A. Lusson, and P. Galtier, "Opposite crystal polarities observed in spontaneous and vapour-liquid-solid grown ZnO nanowires," Applied Physics Letters **102**(18), 182103 (2013).

[21] M. R. Ramdani, J. C. Harmand, F. Glas, G. Patriarche, and L. Travers, "Arsenic Pathways in Self-Catalyzed Growth of GaAs Nanowires," Crystal Growth & Design **13**(1), 91–96 (2013).

[22] Y. Chen, H. Ko, S. Hong, T. Yao, and Y. Segawa, "Two-dimensional growth of ZnO films on sapphire (0001) with buffer layers," Journal of Crystal Growth **214–215**, 87–91 (2000).

[23] K. Iwata, P. Fons, S. Niki, A. Yamada, K. Matsubara, K. Nakahara, and H. Takasu, "Improvement of Electrical Properties in ZnO Thin Films Grown by Radical Source(RS)-MBE," physica status solidi (a) **180**(1), 287–292 (2000).

[24] H. Yuji, K. Nakahara, K. Tamura, S. Akasaka, Y. Nishimoto, D. Takamizu, T. Onuma, S. F. Chichibu, A. Tsukazaki, A. Ohtomo, and M. Kawasaki, "Optimization of the Growth Conditions for Molecular Beam Epitaxy of $Mg_xZn_{1-x}O$ ($0 \leq x \leq 0.12$) Films on Zn-Polar ZnO Substrates," Japanese Journal of Applied Physics **49**(7), 071104 (2010).

[25] S. K. Hong, Y. Chen, H. J. Ko, H. Wenisch, T. Hanada, and T. Yao, "ZnO and related materials: Plasma-Assisted molecular beam epitaxial growth, characterization and application," Journal of Electronic Materials **30**(6), 647–658 (2001).

[26] C. F. Klingshirn, A. Waag, A. Hoffmann, J. Geurts, "Zinc Oxide: From Fundamental Properties Towards Novel Applications", Springer-Verlag Berlin Heidelberg (2010).

[27] J. Y. Park, D. J. Lee, Y. S. Yun, J. H. Moon, B.-T. Lee, and S. S. Kim, "Temperature-induced morphological changes of ZnO grown by metalorganic chemical vapor deposition," Journal of Crystal Growth **276**(1), 158–164 (2005).

[28] N. Izyumskaya, V. Avrutin, W. Schoch, A. El-Shaer, F. Reuß, Th. Gruber, and A. Waag, "Molecular beam epitaxy of high-quality ZnO using hydrogen peroxide as an oxidant," Journal of Crystal Growth **269**(2), 356–361 (2004).